J Mol Model (2007) 13:319–326
DOI 10.1007/s00894-006-0146-7

ORIGINAL PAPER

# Fundamental measure theory of hydrated hydrocarbons

**Victor F. Sokolov · Gennady N. Chuev**

Received: 24 November 2005 / Accepted: 27 June 2006 / Published online: 13 September 2006


**Abstract** To calculate the solvation of hydrophobic solutes, we have developed a method based on the fundamental measure treatment of density functional theory. This method allows us to carry out calculations of density profiles and the solvation energy for various hydrophobic molecules with high accuracy. We have applied the method to the hydration of various hydrocarbons (linear, branched and cyclic). The calculations of the entropic and enthalpic parts are also carried out. We have examined the question of the temperature dependence of the entropy convergence. Finally, we have calculated the mean force potential between two large hydrophobic nanoparticles immersed in water.

**Keywords** Hydrophobic interactions · Solvation energy · Complex formation

**Abbreviations**

| | |
|---|---|
| SPT | scaled particle theory |
| WPI | Widom particle insertion |
| DFT | density functional theory |
| FMT | fundamental measure theory |
| LJ | Lennard-Jones |
| HS | hard sphere |

Proceedings of "*Modeling Interactions in Biomolecules II*", Prague, September 5th–9th, 2005.

V. F. Sokolov (✉) · G. N. Chuev
Institute of Theoretical and Experimental Biophysics,
Russian Academy of Sciences,
Pushchino, Moscow region 142290, Russia
e-mail: vicvor@mail.ru

## Introduction

Membrane formation, protein folding, the stabilization of various biomacromolecular complexes, including nucleic acids and lipids are largely driven by hydrophobic interactions [1, 2]. The main reason is that all these substances contain a large number of nonpolar groups. Hydrophobic hydration describes structural and dynamic changes of water around a single nonpolar solute whereas hydrophobic interactions form a net of intermolecular bonds (e.g. hydrogen bonds for water). This latter effect refers to a tendency of nonpolar solutes to stick together in aqueous solution. The theory of the hydrophobic effect is intrinsically difficult. Despite a long history of research into hydrophobic interactions, there is at present no complete understanding of their nature. The difficult multiscale character of these effects can be revealed as well as microscopic changes of water structure near small hydrophobic groups and conformations or aggregation of biomacromolecules at mesoscopic scales up to several tens of Ångstrøm [3].

Historically, hydrophobicity has been described as low solubility of nonpolar solutes in water in comparison with organic solvents [4]. Hydrophobic hydration has long been regarded as a peculiar type of solvation, since it is characterized by an unfavorable entropy contribution rather than by an unfavorable enthalpy change [4, 5], and iceberg-like models that postulate an increasing water structure around the solute have been invoked to explain this property. It has been specified subsequently that polar solutes also reveal unfavorable hydration entropies [6, 7].

A wide variety of approaches has been used to describe and explain hydrophobic hydration on the molecular level. Earlier approaches such as scaled particle theory (SPT) [8–10] and the methods of the integral equations [11, 12] were

essentially analytical. Later, an increase of the computation capability has been made possible computer simulations of the solvation process [13]. The coupling of such simulations with statistical thermodynamic techniques, such as the free-energy-perturbation method [14] and the Widom particle insertion (WPI) approach [15], provide computation of the free energy of hydration.

The immersion of a solute (e.g. any hydrocarbon) to water strongly modifies its local structure. This effect is very significant and computer simulation is often necessary for its description. Molecular dynamics and Monte Carlo techniques are most frequently used for modeling molecular interactions in solutions [16]. However, their application to the problem of hydrophobic interactions of macromolecules demands huge computing expenses and in some cases is essentially limited because of the multiscale character of these interactions. In the last decades, new methods based on a statistical treatment are in progress [3, 17–20]. In our opinion, the most suitable method for research of the specified effects is density functional theory (DFT) [21, 22]. This approach considers liquids as spatially disorder ensembles and also allows one to calculate solvation effects, using the data about the molecular structure and intermolecular interaction potentials. The basic purpose of approach is to construct the free-energy functional of the system, which depends on density distribution of liquid particles and interaction potentials between solute and solvent molecules. Within the framework of this approach, there are many different models connected with a concrete choice of density functional [23–26]. One of most suitable versions of DFT for the calculation of solvation is fundamental measure theory (FMT) [24, 25, 27, 28]. FMT determines the free-energy functional as the sum of the weighted contributions that depend on the geometrical characteristics of a solvated particle. It automatically results in the definition of weighted functions responsible for the volume and the surface contributions to the solvation energy.

In this work, we will calculate hydrophobic solvation on the basis of FMT. In particular, we will evaluate the size dependence of the excess chemical potential of the solute and calculate the excess chemical potentials for hydrocarbons in water. On the basis of FMT, we will decompose the excess chemical potential into the excess solvation enthalpy and the excess solvation entropy. Moreover, we will estimate the energy of association and the mean force potential between the two solutes within the limit of low concentration of the dissolved particles.

## Fundamental measure theory

Density functional theory (DFT) [21] solves a problem by a search of the free energy for liquids. The free energy consists of two contributions: ideal ($F_{\mathrm{id}}[\rho]$) and excess $F_{\mathrm{ex}}[\rho]$ free energies:

$$F[\rho] = F_{id}[\rho] + F_{ex}[\rho],\ \beta F_{id}[\rho] = \int \rho(\mathbf{r})\ln[\rho(\mathbf{r})\Lambda^3 - 1]d\mathbf{r}, \tag{1}$$

where $\Lambda$ is the De-Broglie wavelength, $\rho(\mathbf{r})$ is local density, $\beta=(k_BT)^{-1}$ is the inverse temperature, and $k_B$ is the Boltzmann constant.

Minimization of the functional leads to the equilibrium density:

$$\rho(\mathbf{r}) = \rho_{\mathrm{b}}\exp[-\beta U_{\mathrm{ext}}(r) + \delta F_{\mathrm{ex}}[\rho]/\delta\rho(\mathbf{r}) - \delta F_{\mathrm{ex}}[\rho_{\mathrm{b}}]/\delta\rho(\mathbf{r})] \tag{2}$$

where $U_{\mathrm{ext}}(r)$ is intermolecular potential, $\rho_{\mathrm{b}}=\rho(\mathbf{r}\to\infty)$ is the bulk density.

Thus, if the functional $F_{\mathrm{ex}}[\rho]$ is known, we can calculate the density profile $\rho(\mathbf{r})$ and then all required characteristics of solvation.

There are many ways of designing the functional $F_{\mathrm{ex}}[\rho]$, most of them use data on functional derivatives $\partial F_{\mathrm{ex}}/\partial\rho(\mathbf{r})$ and $\partial^2 F_{\mathrm{ex}}/\partial\rho(\mathbf{r})\partial\rho(\mathbf{r}')$ of the particle density. One of the methods is FMT [24, 25, 27, 28], which is based on the following representation. It assumes the calculation of the free energy for a non-uniform liquid $F_{\mathrm{ex}}[\rho]$, using the information about a homogeneous liquid $F[\rho_{\mathrm{b}}]$. This is possible since the local density of the non-uniform liquid is practically constant in a microvolume whose size does not surpass the characteristic size of liquid particles. Since the local density is different in various microvolumes, the free energy can be expressed through an integral that depends on the density of the free energy of a non-uniform liquid:

$$\beta F_{\mathrm{ex}}[\rho] = \int \Phi[n_i(\mathbf{r})]d\mathbf{r}, \tag{3}$$

where variables $n_i(\mathbf{r})$ are determined as weights

$$n_i(\mathbf{r}) = \int \rho(\mathbf{r}')w_i(\mathbf{r}-\mathbf{r}')d\mathbf{r}' \tag{4}$$

of the density $\rho(\mathbf{r}')$ averaged with weight factors $w_i(\mathbf{r}-\mathbf{r}')$. Here, index $i$ denotes the number of weight density. These weights are the characteristic functions that determine the geometry of the solute, and in the three-dimensional case they are expressed as:

$$\begin{aligned} &w_3(r) = \Theta(\sigma/2 - r),\ w_2(r) = \delta(\sigma/2 - r),\\ &w_1(r) = w_2(r)/(2\pi\sigma),\ w_0(r) = w_2(r)/(\pi\sigma^2),\\ &\mathbf{w}_{v2}(\mathbf{r}) = \mathbf{r}\delta(\sigma/2 - r)/r,\ \mathbf{w}_{v1}(\mathbf{r}) = \mathbf{w}_{v2}(\mathbf{r})/(2\pi\sigma), \end{aligned} \tag{5}$$

where $\delta(r)$ and $\Theta(r)$ are the Dirac delta-function and the Heaviside function, respectively, $\sigma$ is the diameter of a solvent particle. The weight factors $w_0$, $w_1$, $w_2$, $w_3$ are scalars, $\boldsymbol{w}_{v1}$ and $\boldsymbol{w}_{v2}$ are vectors.

Within the framework [24, 25, 27, 28], the function $\Phi[n_i]$ is determined through weight densities $n_0(\mathbf{r})$–$n_3(\mathbf{r})$, $\boldsymbol{n}_{v1}(\mathbf{r})$ and $\boldsymbol{n}_{v2}(\mathbf{r})$ as

$$\Phi[n_i] = -n_0\ln(1-n_3) + (n_1 n_2 - \boldsymbol{n}_{v1}\boldsymbol{n}_{v2})/(1-n_3) + (n_2^3 - 3n_2\boldsymbol{n}_{v2}\boldsymbol{n}_{v2})/(24\pi(1-n_3)^2). \quad (6)$$

Using Eqs. 2 and 6, we obtain the equilibrium density

$$\rho(\mathbf{r}) = \rho_b \exp\left\{-\beta U_{\text{ext}}(r) + \sum_i \int \{[\delta\Phi(\mathbf{r}) - \delta\Phi(\mathbf{r}' \to \infty)]\delta n_i(\mathbf{r})\} w_i(\mathbf{r}-\mathbf{r}')d\mathbf{r}'\right\}. \quad (7)$$

In turn the excess part of thermodynamic potential $\Delta\mu_{\text{ex}}$ determining the solvation free energy is calculated as

$$\Delta\mu_{ex} = F_{ex} - \sum_i n_i \frac{\delta F_{ex}}{\delta n_i} \quad (8)$$

It is significant that integration of the Eq. 3 for calculation of the excess chemical potential (8) must be carried out from the chosen $r_{\text{cut}}$ to infinity, but not from zero to infinity. The main reason is the fact that FMT theory in origin does not treat pressure correctly. As a result, the excess chemical potential is proportional to the volume of solute and surface part of the excess chemical potential becomes much less than volume part. In this case, we cannot calculate the excess chemical potential correctly. We have found a way to solve this problem. We have chosen the point $r_{\text{cut}}$ so as to predict the experimental surface tension of water 102 cal mol$^{-1}$ Å$^{-2}$. In this case the magnitude of pressure ($\beta p\sigma^3$) is about 0.05. We note that originally the FMT method was advanced for a liquid of hard spheres. The FMT method can be applied to spheroids of rotation [29], and also for various repulsive and attractive potentials [30–32]. In the last case, the attraction part of potential $U_{\text{att}}(r)$ is considered as a perturbation, which gives the contribution to the free energy

$$F_{vv}[\rho] = \frac{1}{2}\iint [\rho(\mathbf{r}) - \rho_b]U_{att}(r)[\rho(\mathbf{r}') - \rho_b]d\mathbf{r}d\mathbf{r}'. \quad (9)$$

When we considered the hard sphere solute dissolved in Lennard-Jones (LJ) water, we had to take into account the solute–solvent attractive interactions. The first order correction of the excess chemical potential is expressed as

$$F_{uv}[\rho] = \rho_b \int g_{HS}(\mathbf{r})U_{att}(r)\,d\mathbf{r}. \quad (10)$$

Since experiments are most commonly done at fixed pressure $\rho$, it is convenient to decompose the hydration chemical potential into the excess solvation entropy $\Delta S$ and the excess solvation enthalpy $\Delta H$, achieved by the use of an isobaric temperature derivative [33–36]

$$\Delta S = \left(\frac{\partial\Delta\mu_{ex}}{\partial T}\right)_p, \qquad \Delta H = \Delta\mu_{ex} + T\Delta S. \quad (11)$$

Information on the weighted densities also allows us to calculate the mean force potential $A_{\text{ass}}(\mathbf{r})$ determining the force of interaction between two solutes in an indefinitely diluted solution

$$A_{ass}(\mathbf{r}) = V_{uu}(\mathbf{r}) - \int \sum_i \{[\delta\Phi(\mathbf{r}') - \delta\Phi(\mathbf{r}' \to \infty)]/\delta n_i(\mathbf{r}')\}\mathbf{w}_i(\mathbf{r}-\mathbf{r}')d\mathbf{r}', \quad (12)$$

where $V_{\text{uu}}(\mathbf{r})$ is the direct intermolecular interaction potential.

## Results and discussion

Using fundamental measure theory, we have calculated the radial distribution functions for linear, branched and cyclic hydrocarbons (methane, ethane, butane and et al.) in water [37]. On the basis of them and Eq. 8, we have evaluated the excess chemical potential for the hydrocarbons in water. The repulsive interaction between solute and solvent molecules with $\sigma = \sigma_v = 2.77$ Å and $\varepsilon_v$=0.1554 kcal mol$^{-1}$ [38] is simulated as hard spheres (HS). The sizes of hydrocarbons $\sigma_u$ and their Lennard-Jones parameters $\varepsilon_u$ were extracted from References [39, 40]. The water density $\rho_b\sigma_v^3$ was equal to 0.7. The calculations of the attractive contribution were carried out in the framework of a perturbation theory to take into account most factors that influence a solvation process. The attractive interactions between solute and solvent molecules were calculated as first order corrections to the excess chemical

potential (10) for attractive part of the Lennard-Jones potential, according to the Weeks–Chandler–Anderson derivation

$$U_{att}(r) = \begin{cases} -\varepsilon_{uv}, r < \sqrt[6]{2}\sigma_{uv}, \\ 4\varepsilon_{uv}\left(\left(\frac{\sigma_{uv}}{r}\right)^{12} - \left(\frac{\sigma_{uv}}{r}\right)^{6}\right), r \geq \sqrt[6]{2}\sigma_{uv} \end{cases} \quad (13)$$

where $\sigma_{uv} = \frac{\sigma_u + \sigma_v}{2}$ and $\varepsilon_{uv} = \sqrt{\varepsilon_u}\varepsilon_v$.

In addition, we have calculated the attractive contribution to the energy of solvent-solvent interactions using Eq. 11. Note that this attractive part of the solvent-solvent energy decreases from 14 to 1% with increasing solute radius from 0.5 to 20 Å. In contrast, the solute–solvent contribution increases with increasing the radius of the solute. The magnitude of the solute–solvent energy is about 50% or more of the excess chemical potential. It is not necessary to calculate the second order of perturbation theory because of the size of hydrocarbons is enough large that this contribution is negligible.

Figure 1 shows the difference between the FMT and experimental results for the excess chemical potentials, enthalpies and entropies of hydrocarbons. The magnitudes of the excess chemical potentials for small hydrocarbons (methane, ethane and propane) are slightly different from the experimental results. However, the difference of the excess chemical potentials for large solutes is more significant. The main reason is that methane, ethane and propane can be easily approximated by hard-sphere solutes without loss of accuracy. In contrast, for a large solute, it is necessary to take into account its molecular structure, although the FMT results are close enough to the experimental ones.

Moreover, we carried out a decomposition analysis of the excess chemical potential for hydrocarbons into entropic and enthalpic parts. Using Eq. 11, we have decomposed the excess chemical potential to two parts $\Delta H$ and $-T\Delta S$. The calculated and experimental excess chemical potential, the enthalpies, and the entropies of the hydrocarbons from methane to hexane, of the branched hydrocarbons isobutane, 2-methylbutane, and neopentane, and of the cyclic hydrocarbons cyclopentane and cyclohexane are shown in Fig. 1. The obvious feature is that the entropic and enthalpic terms are larger in absolute value than the excess chemical potential. The hydration enthalpies are large and favorable, and the hydration entropies are large and unfavorable. The entropic terms are marginally larger in absolute value than the enthalpic terms, resulting in unfavorable but small hydration free energies of the hydrocarbons. It is recognized that this behavior is typical for hydrophobic hydration. Solvation of apolar compounds in most other solvents, in fact, is usually accompanied by smaller enthalpic and entropic changes. Figure 1 shows the difference between the experimental and the calculated enthalpy and entropy parts of the excess chemical potential [41]. The discrepancies in enthalpy do not exceed 7 kcal mol$^{-1}$ for all hydrocarbons (except 2-methylbutane and cyclopentane due

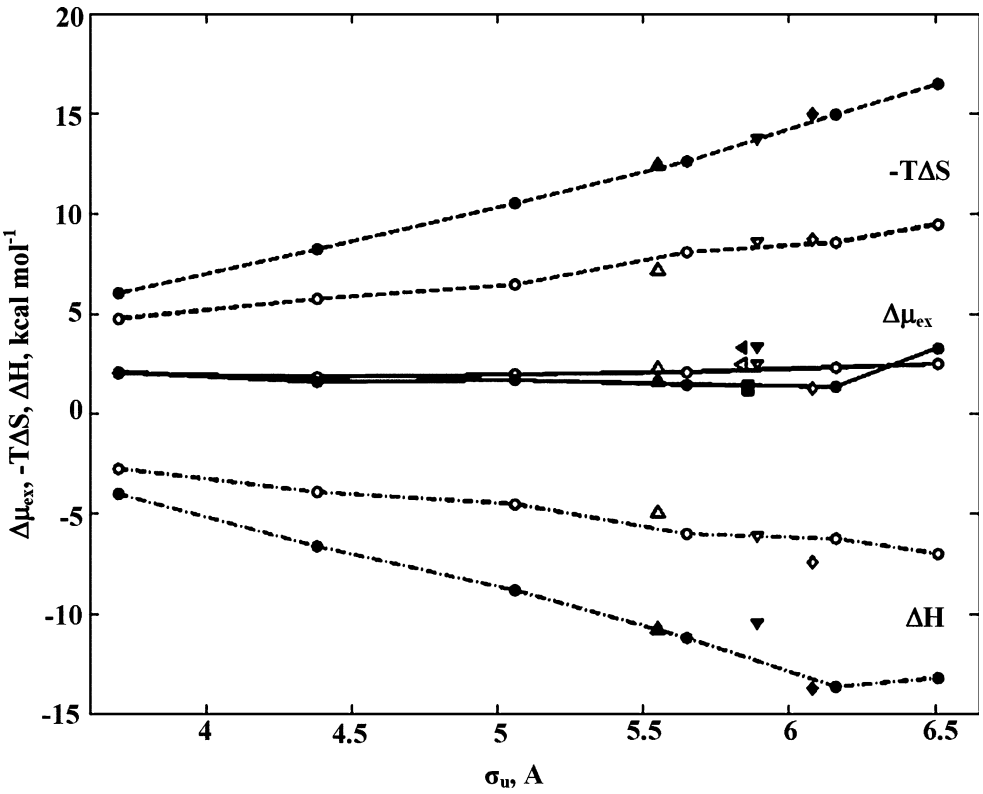


**Fig. 1** The calculated and the experimental excess chemical potentials (*solid lines*), enthalpies (*dash-dotted lines*), and entropies (*dashed lines*) of hydrated alkanes: (*circles*) normal alkanes from $C_1$ to $C_6$ in order of increasing solute diameter; (*triangles-up*) isobutane; (*rotated triangle*) 2-methylbutane; (*triangles-down*) neopentane; (*squares*) cyclopentane; (*diamonds*) cyclohexane

to strong differences of the molecules from spheres). The calculated excess chemical potential of methane is 3% more positive than the experimental value (2.01 kcal $mol^{-1}$). Partially, this difference is due to the fact that the calculated hydration enthalpy of methane is about 3.97 kcal $mol^{-1}$ more negative than experiment (−2.75 kcal $mol^{-1}$). This represents a significant discrepancy if compared to the better agreement between the calculated and the experimental relative hydration enthalpies for the higher alkanes. The calculated hydration entropy of methane, although in better agreement with the

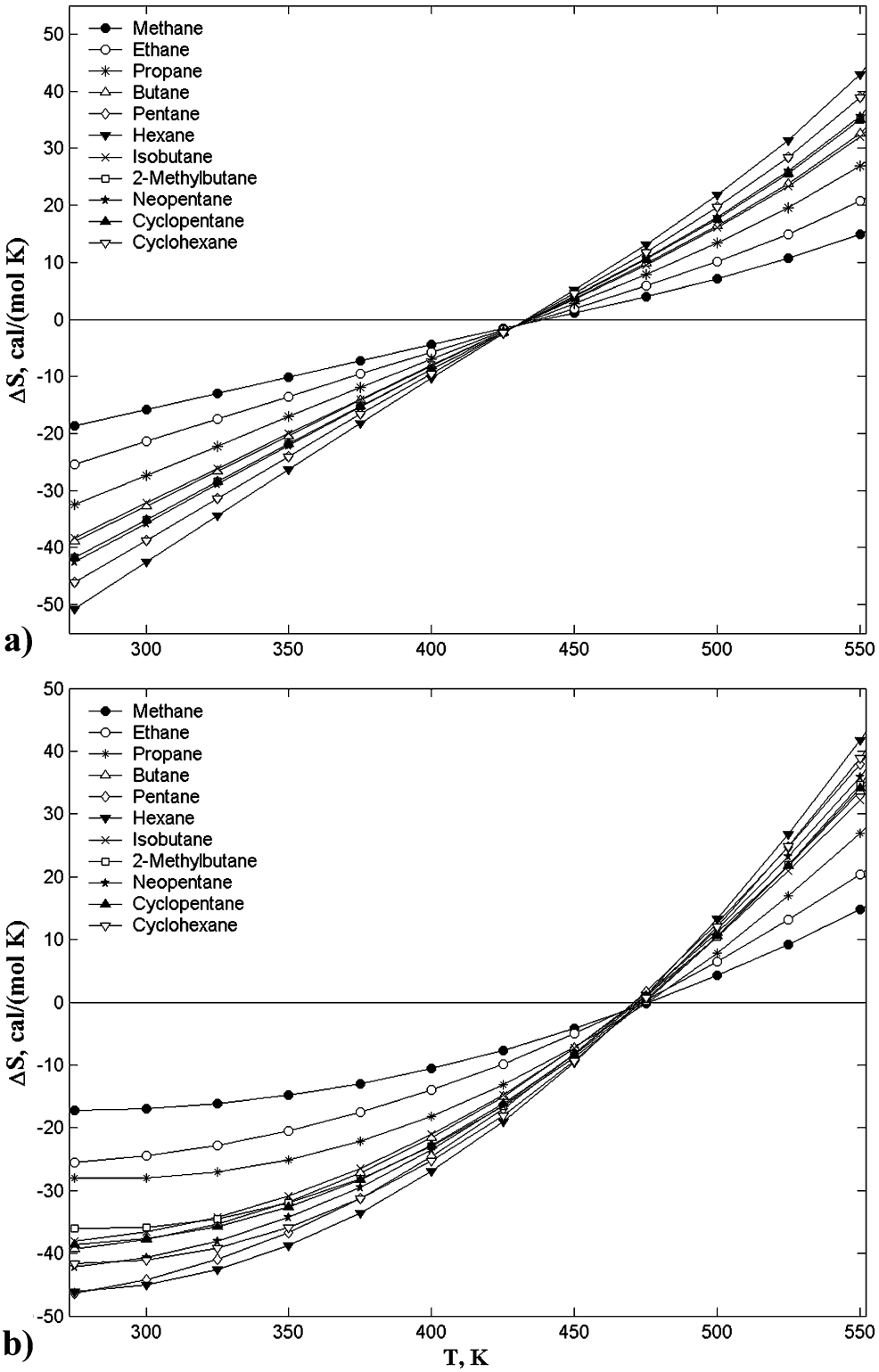


**Fig. 2** Hydration entropy of HS solutes with radii corresponding hydrocarbons (see legend) as a function of temperature along the saturation curve of water. Case **a** corresponds to the water HS diameter independent on temperature, while the case **b** to the water diameter depending on temperature [45]

experimental hydration entropy ($-T\Delta S$=6.04 kcal mol$^{-1}$), is found to be too large. The difference in the enthalpy and entropy partially cancel each other, resulting in a smaller discrepancy in the excess chemical potential. The calculated and experimental hydration free energies of the alkanes are positive and practically do not increase with solute size (Fig. 1).

The decrease in the excess chemical potential going from methane to ethane is well reproduced by the calculations. The calculations overestimate the value of the negative enthalpy change and strongly underestimate the entropy loss in going from methane to ethane. Both effects result in a less favorable hydration free energy of ethane. It appears that the current hydrocarbon model should take into account a larger benefit in favorable hydrocarbon–water interactions in going from methane up to ethane without the further loss of entropy.

The experiments show that each methylation beyond the first increases the free energy of hydration of the linear alkanes by approximately 0.2 kcal mol$^{-1}$, whereas the calculated free energy increase at each methylation is on average a little higher. Unfortunately, the calculations do not reproduce the experimental 1.2 kcal mol$^{-1}$ free-energy difference between hexane and cyclohexane and 1.1 kcal mol$^{-1}$ between cyclopentane and pentane.

The calculated and experimental enthalpies of hydration of the normal alkanes are not in good agreement (Fig. 1). The calculations overestimate the magnitude of the experimental enthalpies of hydration. Despite the quite favorable enthalpies of hydration, the solubility in water of these compounds remains low due to the unfavorable entropies. Unfortunately, the calculated and the experimental enthalpies of hydration of the linear alkanes are also not in good agreement. The experimental entropy losses are underestimated by the calculations. This effect could be partly due to having ignored the torsional degrees of freedom of the carbon chains. For linear alkanes each additional methylation decreases $T\Delta S$ by about 2.0 kcal mol$^{-1}$. The $-T\Delta S$ values are larger in magnitude than the $\Delta H$ values, resulting in the positive hydration free energies discussed above.

The free energies of hydration of the cyclic alkanes favor hydration less than their corresponding linear homologues. The free-energy drop caused by cyclization is reproduced by the calculations, although a little overestimated. It has been shown experimentally and computationally that the solubility of cyclohexane increases with respect to hexane significantly favorable than the expected enthalpy of hydration. Despite their different accessible surface areas, the enthalpies of cyclohexane and hexane are of similar magnitude. The calculations also show that the larger solubility of cyclopentane compared to an alkane of the same solvent accessible surface area is due mostly to a more favorable hydration enthalpy, although partially offset by a more unfavorable entropic component.

The hydrophobic effect is frequently connected to characteristic temperature dependences [42–44]. One of

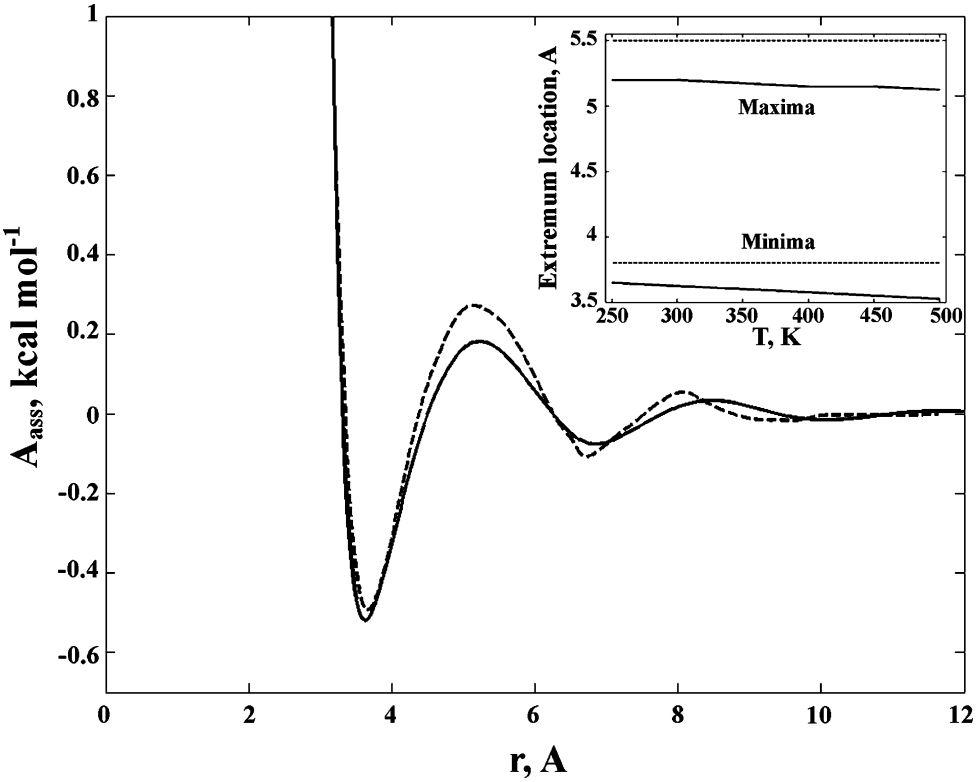


**Fig. 3** The mean force potential $A_{ass}(r)$ of a methane-like solute at 300 K ($\sigma_{uv}$=3.336 Å, $\varepsilon_{uv}$= 0.241 kcal mol$^{-1}$, $\sigma_u$=3.57 Å, $\varepsilon_u$=0.4 kcal mol$^{-1}$). The temperature dependencies of the first minimum and maximum are represented in the *upper-right corner* of the figure

the most surprising observations is the entropy of transition convergence of nonpolar molecules from gas phase or nonpolar solvent into water at a temperature of about 400 K to approximately zero entropy change. We have performed calculations to indicate that FMT is able to predict the temperature convergence of entropy correctly, both qualitatively and quantitatively. Computer simulations were carried out to calculate the water-oxygen radial distribution function $g(r)$ and the excess chemical potential for hydrocarbons at several temperatures along the experimental saturation curve of water.

Using Eq. 11, we have obtained the solvation entropy by calculating the derivative of the chemical potential along the saturation curve. Figure 2 shows the temperature dependence of the entropy $\Delta S$ for the different solutes for two cases of calculation. In the first case (Fig. 2a) we calculated the excess chemical potential without the fact that the diameter of water decreases with increasing temperature. The entropies are large and negative at room temperature for all the solutes and decrease in magnitude with increasing temperature. The temperature dependence of the entropies is approximately linear with slopes increasing with increasing solute size. Moreover, the entropies converge at about 400 K to approximately zero entropy, although at closer inspection the temperature range of the convergence region is several 10 K and the entropy is not exactly zero at convergence. In the second case, we have taken into account the dependence of the solvent diameter on temperature [45]. Figure 2b shows that the point of entropy convergence has shifted to region where temperature and entropy magnitude is about 470 K and $-2.5$ cal mol$^{-1}$ K$^{-1}$, correspondingly. The convergence region has become a little wider. It is significant that taking into account the contributions of solute–solvent interactions has changed both the point of entropy convergence (about 500 K) and the width of convergence region.

We must note the one more benefit of fundamental measure theory. The theory allows the calculation of the mean force potential between two solutes surrounded with solvent particles. In this work, we have obtained the profiles of mean force potentials of different solutes at various temperatures. An example of such a curve is plotted in Fig. 3. The dependence of the location of maxima and minima on temperature is plotted in the upper-right corner of Fig. 3. Figure 3 shows that the extrema of mean force potential move linearly to left with increasing temperature. In reality, the localization of extrema practically does not change with increasing temperature. The reason for the discrepancy between calculated and simulation results is a small error in the FMT calculations. The magnitude of the potential barrier obtained by FMT is a little underestimate in the simulation result (about 0.1 kcal mol$^{-1}$).

## Conclusions

In this work we used fundamental measure theory for a quantitative description of hydrophobic phenomena based on density functional theory. As a result, we have obtained profiles of radial distribution functions for the isolated solutes (hydrocarbons) in hard sphere fluids. Using the profile of a distribution function, in the framework of FMT we have calculated the excess chemical potentials for linear, branched and cyclic hydrocarbons in water by modeling them as spherical solutes. The water molecules were modeled as LJ solvent. In addition, we have derived the excess chemical potentials for hydrocarbons and their entropic and enthalpic parts. The differences between experiment and the FMT results are not large for hydration free energy and more significant for entropy and enthalpy. Moreover, we have calculated the mean force potential for methane-like solute and have shown the changing the extrema with increasing temperature.

**Acknowledgment** This work was partly supported by the Russian Foundation of Basic Research.

## References

1. Tanford C (1973) The hydrophobic effect formation of micelles and biological membranes. Wiley, New York
2. Ben-Naim A (1980) Hydrophobic interactions. Plenum, New York
3. Lum K, Chandler D, Weeks JD (1999) J Phys Chem B 103:4570–4577
4. Ben-Naim A (1974) Water and aqueous solutions. Plenum, New York
5. Abraham MH (1982) J Am Chem Soc 104:2085–2094
6. Ben-Naim A, Marcus Y (1984) J Chem Phys 81:2016–2027
7. Pierroti RA (1976) Chem Rev 76:717–726
8. Reiss H, Frisch HL, Lebowitz JL (1959) J Chem Phys 31:369–380
9. Pierroti RA (1965) J Phys Chem 69:281–288
10. Wilhelm E, Battino R (1972) J Chem Phys 56:563–566
11. Pratt LR, Chandler D (1977) J Chem Phys 67:3683–3704
12. Pratt LR, Chandler D (1980) J Chem Phys 73:3430–3433
13. Allen MP, Tildesley DJ (1987) Computer simulations of liquids. Clarendon, Oxford
14. Zawanzig RW (1954) J Chem Phys 22:1420–1426
15. Widom B (1982) J Phys Chem 86:869–872
16. Frenkel D, Smit B (1996) Understanding molecular simulation: from algorithms to applications, 1st edn. Academic, New York
17. Hummer G, Garde S, Garcia AE, Pratt LR (2000) J Chem Phys 258:349–370
18. Pratt LR, Pohorille A (2002) Chem Rev 102:2671–2692
19. Huang DM, Chandler D (2002) J Phys Chem B 106:2047–2053
20. Alexandrovsky VV, Basilevsky MV, Leontyev IV, Mazo MA, Sulimov VB (2004) J Phys Chem B 108:15830–15840
21. Evans R (1992) In: Henderson D (ed) Fundamentals of inhomogeneous fluid, Wiley, New York
22. Barrat JL, Hansen JP (2003) Basic concepts for simple and complex liquids. Cambridge University Press, Cambridge
23. Curtin WA, Ashcroft W (1985) Phys Rev A 32:2909–2919
24. Rosenfeld Y (1989) Phys Rev Lett 63:980–983

25. Rosenfeld Y, Schmidt M, Löwen H, Tarazona P (1997) Phys Rev E 55:4245–4263
26. Tarazona P (1985) Phys Rev A 31:2672–2679
27. Löwen H (2002) J Phys Condens Matter 14:11897–11905
28. Schmidt M (2003) J Phys Condens Matter 15:S101–S106
29. Rosenfeld Y (1994) Phys Rev E 50:R3318–R3321
30. Schmidt M (2000) Phys Rev E 62:3799–3802
31. Sweatman MB (2002) J Phys Condens Matter 14:11921–11932
32. Ravikovitch PI, Vishnyakov A, Neimark AV (2001) Phys Rev E 64:011602-1–011602-20
33. Yu HA, Karplus M (1988) J Chem Phys 89:2366–2379
34. Yu HA, Roux B, Karplus M (1990) J Chem Phys 92:5020–5033
35. Garisto F, Kusalik PG, Patey GN (1983) J Chem Phys 79:6294–6300
36. Ben-Naim A, Marcus Y (1984) J Chem Phys 81:2016–2027
37. Chuev GN, Sokolov VF, Phys Rev E (2006) (to be published)
38. Floris FM, Silmi M, Tani A, Tomasi J (1997) J Chem Phys 107:6353–6365
39. Ashbaugh HS, Paulaitis ME (2001) J Am Chem Soc 123:10721–10728
40. Graziano G (2002) Can J Chem 80:401–412
41. Cabani S, Gianni P, Mollica V, Lepori L (1981) J Solution Chem 10:563–595
42. Baldwin RL (1986) Proc Natl Acad Sci USA 83:8069–8072
43. Dill KA (1990) Science 250:297–298
44. Hummer G, Garde S, Garcia AE, Paulaitis ME, Pratt LR (1998) J Phys Chem B 102:10469–10482
45. Graziano G, Lee B (2003) Biophys Chem 105:241–250